Analysis of quantitative MT using principal component analysis

M. Cercignani[1], M. Symms[1], R. Samson[1], M. Yogarajah[1], M. Ron[1], and G. Barker[2]
[1]Institute of Neurology, UCL, London, England, United Kingdom, [2]Institute of Psychiatry, KCL, London, England, United Kingdom

Introduction

Quantitative magnetization transfer (MT) is based on a two-pool model of MT [1], and yields several indices, reflecting properties of the macromolecular pool. The relationship between these indices, and the amount of overlapping information they contain, is not clear, and the interpretation of white matter changes measured by quantitative MT is not always straight-forward. Principal component analysis (PCA) can be used both to reduce the dimensionality of data by reorienting them so that the first few dimensions account for as much of the variance as possible, and to gain insight into patterns of association between variables. Here we use PCA to aid interpretation of quantitative MT parameters.

Methods

This work is based on the model of quantitative MT developed by Ramani et al. [2]. In Ramani's model, the MT pulse is replaced by continuous wave irradiation with the same mean square amplitude (continuous wave power equivalent approximation). Seven quantities can be derived from the model: RM_0^A, f, T_2^A, T_2^B, T_1^A, T_1^B and gM_0^A. Here A and B label the liquid and the macromolecular pools, respectively, R is the exchange rate, f represents the bound proton fraction, M_0^A is the longitudinal magnetization of pool A at the equilibrium, and gM_0^A is the signal measured in the absence of MT saturation [2]. The seven parameters can be uniquely determined only if T_1 of the system is ascertained independently, thus expressing T_1^A as a function of the other parameters [1]. T_1^B is generally fixed to be 1 s [1-3]. Eight subjects (M/F=2/6, median age = 52.5 yrs, range=18-62 yrs) were scanned on a 3.0 T system using a 3D MT-weighted fast SPGR sequence (**A**) (TR/TE=25.8/2.7 ms, flip angle=5º, Gaussian MT pulses, duration=14.6 ms), which collects 11 volumes with various combinations of amplitude (ω) and offset frequency (Δ) of the MT pulse, optimised according to [4]. In addition to the MT data, (**B**) two 3D fast recovery FSE (TR/TE=300/24.3 ms, ETL=12, flip angles=60º and 120º, matrix=64x64), (**C**) 2 fast 3D SPGRs (TR/TE1/TE2=25.8/2.7/5.4 ms, flip angle 5º) and (**D**) 3 fast 3D SPGRs (TR/TE=6.0/2.8 ms, flip angles 15º, 7º,and 3º, #slices=88, slice thickness = 2 mm) were obtained. Images were collected in the coronal plane. Acquisition matrix (256x96), FoV (24x18 cm^2), number of slices (34) and slice thickness (5 mm) were the same for all sequences unless otherwise specified. After image co-registration, B_1 maps were obtained from sequence B using the double angle method [5] and B_0 maps were obtained from sequence C [6]. T_1 maps were calculated from sequence D as described in [3]. Ramani's model was then fitted to the data as in [3], correcting ω and Δ based on the field maps. The 15˚ flip angle SPGR from sequence D was segmented into white matter, grey matter and CSF using SPM99 (www.fil.ion.ucl.ac.uk/spm/). White and grey matter segments were then combined to produce a brain mask to remove CSF. The brain-extracted images were processed using a local-developed algorithm for voxel-based PCA implemented in Matlab (The Mathworks, MA, USA), producing maps of the principal components (PCs), eigenvalues (i.e. the variances associated with each principal component), and component loadings (i.e. the correlation matrix of the principal component scores with the original data) for the system. Five variables were entered into the PCA: f, RM_0^A, T_1^A, T_2^A, and T_2^B.

Results

Maps of the PCs averaged across subjects after normalisation are shown in Fig 1. The eigenvalues for the system were, in descending order: [2.26,1.01,0.86,0.51,0.36]. Using the scree plot [7] we retained the first 3 components, which explain 82.6% of the total variance. The loadings for the first three components are reported in Table 1.

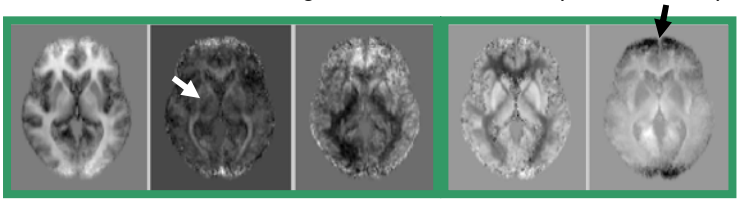

Fig 1. Average PC maps in descending order.

Table 1. PC loadings.
Absolute values>0.5 are highlighted.

	PC1	PC2	PC3
f	**0.77**	0.11	-0.43
RM_0^A	**0.54**	-0.27	**0.77**
T_1^A	**-0.87**	-0.07	0.02
T_2^A	**-0.76**	-0.29	0.00
T_2^B	0.23	**-0.91**	-0.28

Discussion

The principal component loadings suggest that T_1^A and T_2^A, are highly correlated. This is not surprising as most of the variance is likely to come from grey-to-white matter contrast. Similarly, f appears to be correlated with the first PCA component. T_1 is known to be affected by the presence of myelin in white matter [8], and f is believed to reflect the myelin content. Consequently, some (inverse) correlation between f and T_1^A is to be expected and has been previously observed. T_2^B appears to be independent of the other variables and almost entirely summarized by the second component, consistent with the results of Sled et al. [9], who interpeted it as a measure of the rigidity of the structure. The second component contains some interesting features such as contrast between white matter structures running within the axial plane and those running in the superior-inferior direction (white arrow). The third component is mainly represented by RM_0^A, with some weighting from f (thus suggesting that f conveys more information than T_1 alone). A limitation of this type of analysis is the inability to separate variance components genuinely related to the underlying tissue characteristics from those due to image artefacts (see black arrow, pointing at artifact due to FoV edge, as the acquisition was coronal, and low frequency variation on PCs 1 and 2, which might reflect some spatial inhomogeneity of the input maps). A rotated solution might help in removing this ambiguity. It is also interesting to note that the fourth component is characterised by some asymmetry between left and right, which might be related to the $B_1^{(+)}/B_1^{(-)}$ inbalance occurring at high field strength [10].

References

[1] Henkelman RM et al. Magn Reson Med 29 (1993) 759-66.
[2] Ramani A et al. Magn Reson Imaging 20 (2002) 721-31.
[3] Cercignani M et al. NeuroImage 27 (2005) 436-41.
[4] Cercignani M & Alexander DC. Magn Reson Med 56 (2006) 803-10.
[5] Stollberger R & Wach P. Magn Reson Med 35 (1996) 246-51.
[6] Cusack R & Papadakis N. NeuroImage 16 (2002) 754-64.
[7] Cattel RB. Multivariate Behavioral Research 1 (1966) 245-76.
[8] Koenig SH et al. Magn Reson Med 20 (1991) 285-91.
[9] Sled JG et al. Magn Reson Med 51 (2004) 299-303.
[10] Hoult DI. Concepts in Magnetic Resonance 12 (2000) 173-187.